Parabolic Image-Motion*

MILTON D. ROSENAU, JR., *Senior Physicist,*
The Perkin-Elmer Corp., Norwalk, Conn.

ABSTRACT: *Transverse scanning panoramic aerial cameras have a residual image-motion despite optimum image-motion compensation (IMC). This image-motion results from the finite slit width which precludes the film's IMC from being exactly correct for all images simultaneously exposed in the slit. The image displacement is a parabolic function of time, and is also proportional to the film's transport (or scanning) velocity, the airplane's v/h rate, and the sine of the transverse scan-angle; and the modulation transfer-function and phase-shift for this image-motion are evaluated. The potential improvement in the modulation transfer function, which can be achieved by matching the film's IMC velocity to the image's velocity at the middle of the slit rather than at a slit jaw, is illustrated with an example in which the transfer function is raised from 0.68 to 0.98 at 40 cyc/mm. Points forward and aft of the optical axis are shown to have image-motion which is also parabolic, but there is a greater amount of image-displacement for these images than for those imaged on the optical axis.*

INTRODUCTION

INTEREST in transverse-scanning panoramic aerial cameras has stimulated considerable analysis of their performance characteristics. It recently became apparent that one form of image-motion—parabolic displacement as a function of time—arises from finite slit-width. This paper describes the origin of the problem, derives the modulation transfer function, and illustrates the result by considering the performance of the Model 501 Lightweight Aerial Panoramic Camera. Then, off-axis effects are studied, and, in conclusion, general design implications are discussed.

Two forms of transverse-scanning panoramic aerial cameras have been designed: The first has film fixed upon a cylindrical focal surface and sweeps the image across the film by swinging the lens itself; the second has a fixed lens and slit arrangement, accomplishing the transverse scan by rotating a mirror or prism in front of the lens and synchronizing this with the motion of the film past the slit. While parabolic image-motion exists in both forms, only the second form is considered in this article.

THE ORIGIN OF THE PROBLEM

In a transverse-scanning panoramic camera, the image of a flat earth has a forward velocity, $\dot{y}_i$, expressed by

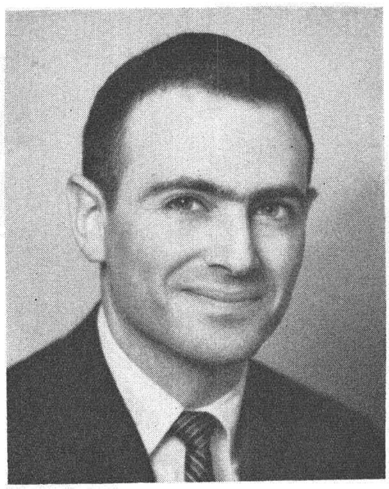

MILTON D. ROSENAU, JR.

$$\dot{y}_i = f\left(\frac{v}{h}\right)\cos\beta, \qquad (1)$$

where f is the effective focal-length, v/h is the ratio of aircraft velocity, relative to the earth, divided by the altitude above the earth (assuming the flight path to be straight and level), and β is the scan-angle, which is the angle between the local vertical from the aircraft and the optical axis projected to the object point being imaged. This relationship is

* Presented at the Society's 27th Annual Meeting, The Shoreham Hotel, Washington, D. C., March 19–22, 1961.

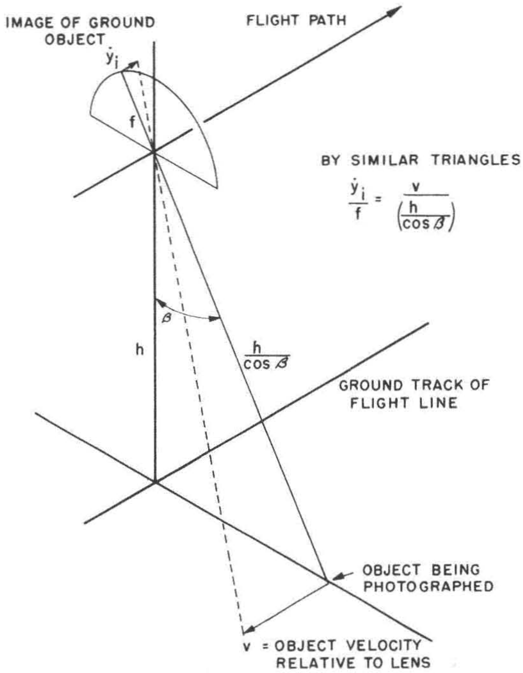

FIG. 1. The geometry of image motion.

illustrated in Figure 1.

Now, it is customary in these cameras to impart a compensating movement to the film so that the photograph will not be blurred by this image movement. This is generally called image-motion compensation (*IMC*). The most rudimentary form of this *IMC* is to merely move all the film forward (or the lens rearward) during the exposure interval with a velocity, $\dot{y}_f$, which is equal to the image velocity. That is,

$$\dot{y}_f = \dot{y}_i. \tag{2}$$

Since transverse-scanning panoramic cameras continuously scan to cover all ground object points perpendicular to the flight line, *IMC* rate constantly varies with varying scan-angle, β.

Unfortunately, therefore, *IMC* is not perfect since the image forming process encompasses a finite time interval. Thus the exposure of a single image point on the film, which should have a single value of $\dot{y}_f$ (equal to $\dot{y}_i$), occurs while the *IMC* mechanization is giving the film a continuum of $\dot{y}_f$. That is,

$$\dot{y}_f = f\left(\frac{v}{h}\right)\cos\delta, \tag{3}$$

where δ is not always equal to β.

Figure 2 illustrates the problem. If we photograph an object at a scan-angle β, its exposure starts when the optic axis crosses the left slit jaw with $\delta = \beta$, but then continues, as the image moves into the slit opening. However, the film's forward velocity changes because the optical axis remains imaged on the left slit jaw and the camera's nominal scan-angle changes continuously to values δ where $\delta \neq \beta$. Furthermore, there is a small change in effective focal-length during the exposure.

If we assume that the slit-width, d, is sufficiently small that its angular-width, d/f, is small, then we can express δ as

$$\delta = \beta - \frac{s}{f}, \tag{4}$$

where

$$0 \leq s \leq d. \tag{5}$$

Now, the image blur rate, $\dot{y}$, is

$$\dot{y} = \dot{y}_f - \dot{y}_i. \tag{6}$$

Substituting equations (1) with a correction for effective focal-length, and (3) and (4) in (6), we get

$$\dot{y} = f\frac{v}{h}\left(\cos\beta\cos\frac{s}{f} + \sin\beta\sin\frac{s}{f} - \frac{\cos\beta}{\cos\frac{s}{f}}\right). \tag{7}$$

Since the angular width of the slit is assumed small,

$$\cos\frac{s}{f} \cong 1, \tag{8}$$

$$\sin\frac{s}{f} \cong \frac{s}{f} \tag{9}$$

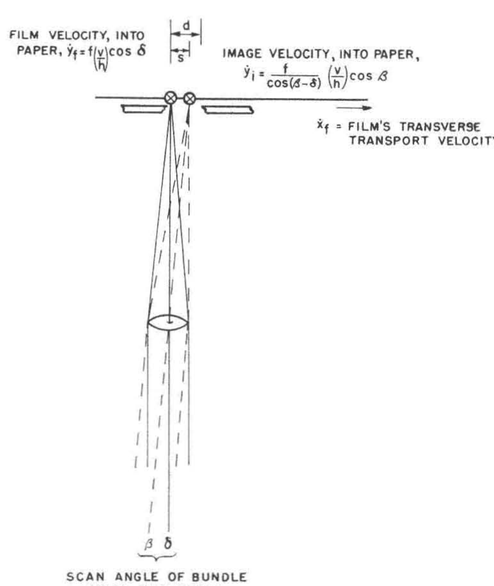

FIG. 2. Geometry of velocity error.

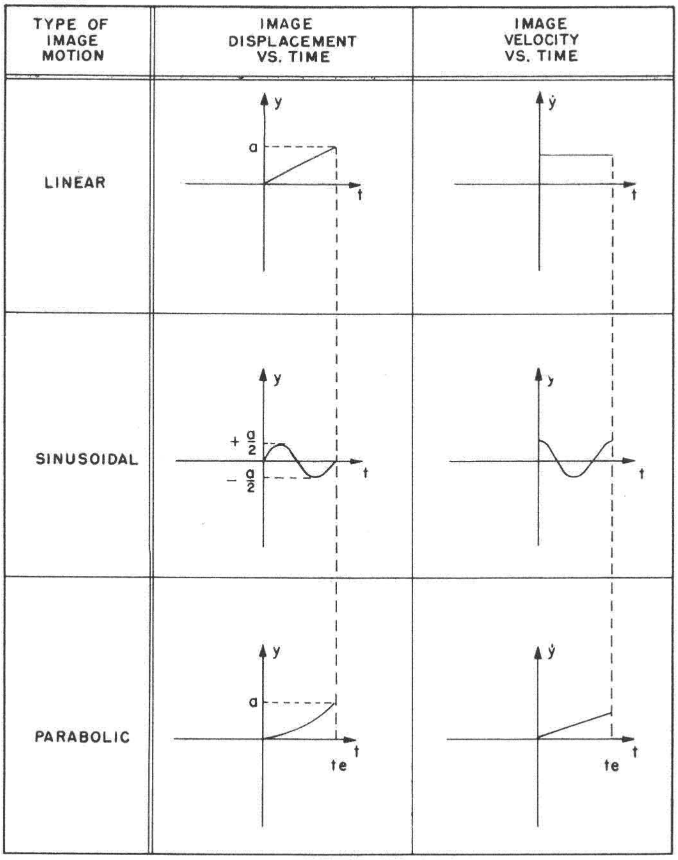

FIG. 3. Comparison of parabolic image motion with linear and sinusoidal image motion.

and therefore

$$\dot{y} = \left(\frac{v}{h}\right) s \sin\beta. \qquad (10)$$

Furthermore, since the film is being transported perpendicular to the slit (to match the transverse scan) with velocity x_f, then the distance s can be expressed as

$$s = t\dot{x}_f, \qquad (11)$$

where

$$0 \leq t \leq t_e, \qquad (12)$$

where t_e is the exposure time and

$$d = t_e\dot{x}_f. \qquad (13)$$

The amount of actual image-blur which has occurred during a part of the exposure, t, is

$$y = \int_0^t \dot{y}dt$$

$$= \left[\frac{1}{2}\left(\frac{v}{h}\right)\dot{x}_f \sin\right] t^2, \qquad (14)$$

and the total image movement, a, during the entire exposure is

$$a = \left[\frac{1}{2}\left(\frac{v}{h}\right)\dot{x}_f \sin\right] t_e^2. \qquad (15)$$

We can call this form of image-motion parabolic-image motion by analogy with what Scott[1] calls linear and sinusoidal image-motion. This is illustrated in Figure 3.

DERIVATION OF THE TRANSFER FUNCTION

Consider the sine-wave intensity distribution shown in Figure 4. If this wave moves during a time interval, then its time integrated resultant has a new modulation. The ratio of these modulations is the transfer function due to that motion. If the sine wave has 100% modulation initially, then the algebraic function expressing the resultant

[1] Scott, R. M., *Photographic Science & Engineering*, 3: 201 (1959).

wave's modulation is the motions transfer function directly.

If the wave has 100% modulation, its initial form can be expressed as

$$I(y, 0) = I_0\left(1 + \cos 2\pi \frac{y}{y_0}\right) \qquad (16)$$
$$= I_0(1 + \cos 2\pi ky)$$

where y_0 is the spatial period and k is the spatial frequency. At time t it can be expressed as

$$I(y, t) = I_0\left(1 + \cos 2\pi \frac{y - \Delta y}{y_0}\right)$$
$$= I_0\left\{1 + \cos\left[2\pi ky - 2\pi ak\left(\frac{t}{t_e}\right)^2\right]\right\}, \qquad (17)$$

since

$$\Delta y = \left[\tfrac{1}{2}\ddot{x}_f\left(\frac{v}{h}\right)\sin\beta\right]t^2$$
$$= a\left(\frac{t}{t_e}\right)^2. \qquad (18)$$

The resultant wave is, of course, the time integrated intensity, or exposure, and this is

$$E(y) = \int_0^{t_e} I(y, t)dt$$
$$= I_0 \int_0^{t_e}\left\{1 + \cos 2\pi ky \cos 2\pi ak\left(\frac{t}{t_e}\right)^2 + \sin 2\pi ky \sin 2\pi ak\left(\frac{t}{t_e}\right)^2\right\}dt. \qquad (19)$$

If we let

$$V = \frac{2}{t_e}\sqrt{ak}\,t, \qquad (20)$$

then

$$2ak\left(\frac{t}{t_e}\right)^2 = \frac{\pi}{2}V^2, \qquad (21)$$

and

$$dt = \frac{t_e}{2\sqrt{ak}}dV, \qquad (22)$$

so that equation (19) can be rewritten

$$E(y) = I_0t_e\left\{1 + \frac{1}{2\sqrt{ak}}\left[\cos 2\pi ky \int_0^{2\sqrt{ak}} \cdot \cos\frac{\pi}{2}V^2dV + \sin 2\pi ky \int_0^{2\sqrt{ak}} \sin\frac{\pi}{2}V^2dV\right]\right\}. \qquad (23)$$

Now, let

$$A = \int_0^{2\sqrt{ak}} \cos\frac{\pi}{2}V^2dV \qquad (24)$$

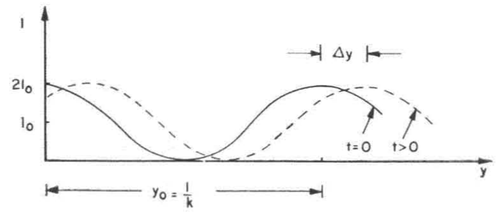

FIG. 4. The intensity sine wave.

and

$$B = \int_0^{2\sqrt{ak}} \sin\frac{\pi}{2}V^2dV, \qquad (25)$$

where A and B are classical functions, Fresnel's cosine and sine integrals, which are tabulated,[2,3] and are functions of ak only. Finally, we can write equation (23) as

$$E(y) = I_0t_e\left\{1 + \frac{1}{2\sqrt{ak}}[A\cos 2\pi ky + B\sin 2\pi ky]\right\}$$
$$= I_0t_e\left\{1 + \frac{\sqrt{A^2+B^2}}{2\sqrt{ak}}\cos(2\pi ky - \theta)\right\}, \qquad (26)$$

where θ is the phase shift due to the parabolic image-motion and is

$$\theta = \cos^{-1}\frac{A}{\sqrt{A^2+B^2}} \qquad (27)$$

In equation (26), the amplitude of the resultant wave is a function of ak alone and thus the transfer function is

$$T(k) = \frac{E_{\max} - E_{\min}}{E_{\max} + E_{\min}}$$
$$= \frac{\left[1 + \frac{\sqrt{A^2+B^2}}{2\sqrt{ak}}\right] - \left[1 - \frac{\sqrt{A^2+B^2}}{2\sqrt{ak}}\right]}{\left[1 + \frac{\sqrt{A^2+B^2}}{2\sqrt{ak}}\right] + \left[1 - \frac{\sqrt{A^2+B^2}}{2\sqrt{ak}}\right]}$$
$$= \frac{\sqrt{A^2+B^2}}{2\sqrt{ak}}. \qquad (28)$$

For large values of ak, A and B approach 0.5, thus

$$\lim_{ak\to\text{large}} T(k) = \frac{.3535}{\sqrt{ak}}, \qquad (29)$$

and

$$\lim_{ak\to\text{large}} \theta = 45°. \qquad (30)$$

[2] Jenkins, F. A. and H. E. White, *Fundamentals of Optics*, 2nd Edition, McGraw-Hill, New York (1950) p. 363.

[3] Jahnke, E. and F. Emde, *Tables of Functions with Formulae and Curves*, 4th Edition, Dover, New York (1945) p. 34.

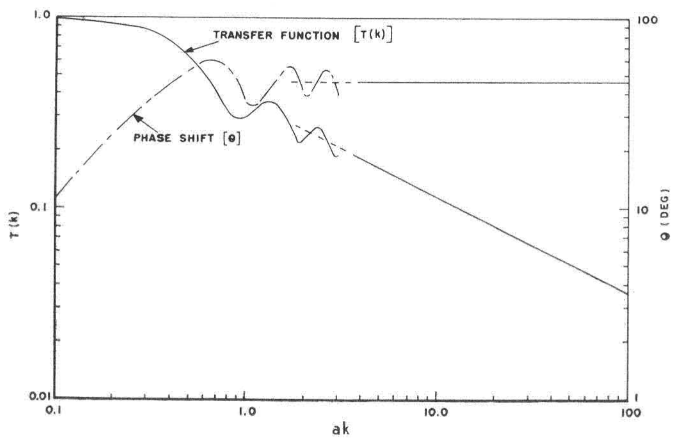

FIG. 5. Normalized transfer function and phase shift for parabolic image motion

The normalized transfer function and phase shift are plotted in Figure 5.

AN ILLUSTRATIVE EXAMPLE

The Model 501 Lightweight Aerial Panoramic Camera operated at maximum v/h rate (0.30 rad/sec) and exposure time (1/55 sec) has a film transport velocity of 10.4 in./sec.[4] Thus, if the scan-angle for which *IMC* is provided is defined by the projection of one slit jaw, we find by equation (15) that, at 60° scan-angle,

$$a = \frac{1}{2}(0.3)(10.4 \times 25.4)(0.866)\left(\frac{1}{55}\right)^2$$
$$= 0.0113 \text{ mm.} \qquad (31)$$
$$= \frac{1}{88} \text{ mm.}$$

Consequently, at its maximum resolution, 40 cyc/mm.,

$$ak = \left(\frac{1}{88}\right)(40) = 0.45, \qquad (32)$$

and

$$T(k) = 0.68. \qquad (33)$$

That is, for scan-angles above 60° from nadir, there is at least a 32% loss of contrast due to parabolic image-motion, if the camera's *IMC* is designed in this fashion.

However, consider the case in which the film velocity is made to match the image velocity in the middle of the slit opening. The amount of image-motion in either half of the slit is

$$a' = \tfrac{1}{4}a. \qquad (34)$$

and

$$a'k = \tfrac{1}{4}ak = 0.11, \qquad (35)$$

so

$$T(k) = .98. \qquad (36)$$

and there is now only a 2% loss of contrast whereas the previous design had a 32% loss of contrast. This is illustrated in Figure 6, and it is clear how a knowledge of this effect has led to a significant improvement in performance.

OFF-AXIS EFFECTS

Figures 7 and 8 illustrate the geometrical problem involved when we consider an off-axis point, such as point A, instead of a point, such as O, which is on the optical axis at the time when the film's *IMC* velocity and the image's velocity are equal. While the off-axis point also has perfect compensation at this instant, its blur velocity at a slightly different time (shown by broken lines in Figures 7 and 8) is greater than that for the axial point, O. This results from the fact that the effective focal length, f, is changing, and this introduces an additional component of image-velocity for off-axis points.

From Figure 8A

$$\begin{aligned} f' &= f \sec(\beta - \beta') \\ &= f \sec(\dot{\beta}t'), \end{aligned} \qquad (37)$$

where $\dot{\beta}$ is the scan rate. Also,

$$\dot{f}' = \frac{df'}{dt'} = f\dot{\beta}\tan(\dot{\beta}t')\sec(\dot{\beta}t'). \qquad (38)$$

The image velocity of point A, $\dot{y}_{i\alpha}$, is

$$\dot{y}_{i\alpha} = f'\frac{V}{h\sec\beta} - \dot{f}'\tan\alpha', \qquad (39)$$

[4] Cowles, C. D. and J. Cohen, *Photographic Sciences & Engineering, 1:* 161 (1958).

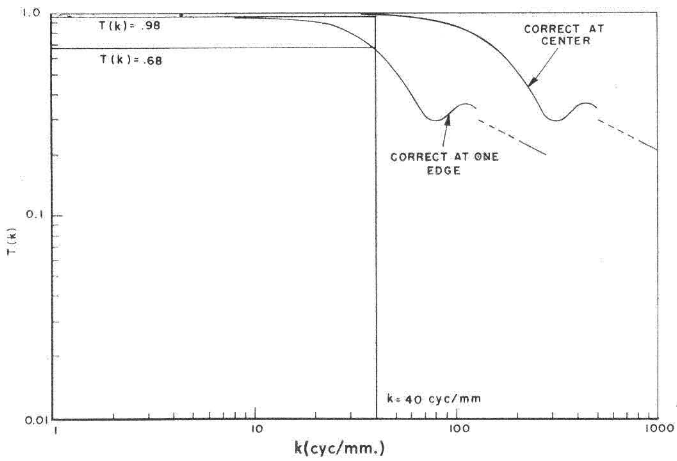

FIG. 6. The effects of making the film's IMC velocity equal to the image velocity in the center of the slit rather than at one edge of the slit in the Model 501 Camera.

whereas the film's *IMC* velocity, $\dot{y}_f$, remains

$$\dot{y}_f = f\left(\frac{v}{h}\right)\cos\beta'. \tag{40}$$

Under the previous assumptions of a small angular slit-width, and further assuming that point A is sufficiently far off-axis so that $D \gg Vt'$, the image blur rate for an off-axis point, $\dot{y}_\alpha$, is

$$\begin{aligned}\dot{y}_\alpha &= \dot{y}_f - \dot{y}i_\alpha \\ &= \left\{f\left(\frac{v}{h}\right)\cos(\beta - \dot{\beta}t')\right\} \\ &= \left\{f\sec(\dot{\beta}t')\left(\frac{v}{h}\right)\cos\beta - f\dot{\beta}\tan(\dot{\beta}t')\sec(\dot{\beta}t') \right. \\ &\qquad \left. \cdot\left[\tan\alpha - \frac{Vt'}{h\sec\beta}\right]\right\} \\ &\cong f\left(\frac{v}{h}\right)\sin\beta\dot{\beta}t' + f\dot{\beta}^2t'\tan\alpha. \end{aligned} \tag{41}$$

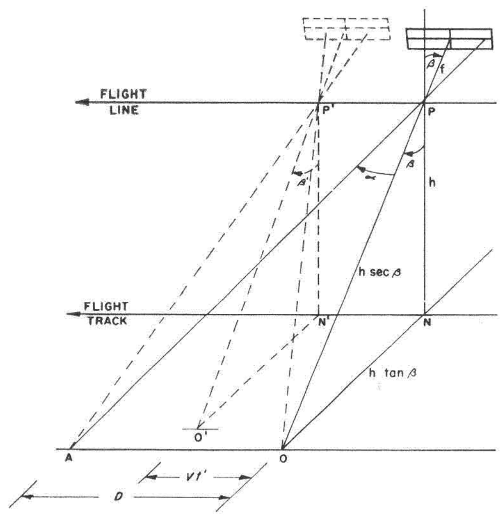

FIG. 7. Isometric view of off-axis geometry.

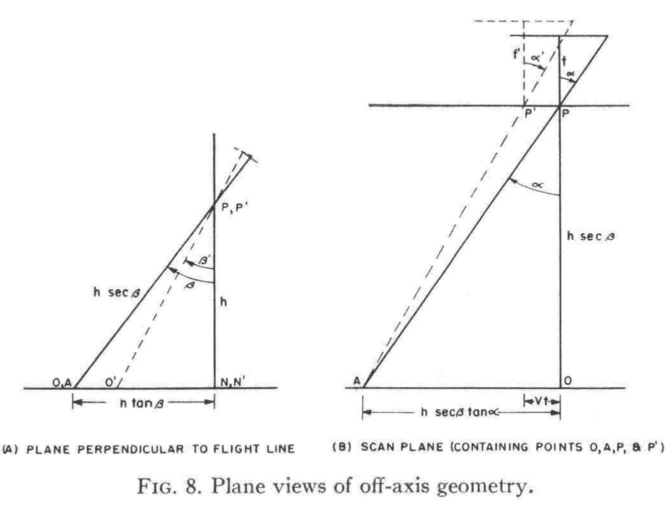

FIG. 8. Plane views of off-axis geometry.

Noting that

$$\dot{x}_f = f\dot{\beta}, \tag{42}$$

we can drop the prime on t, substitute (42) in (41) and obtain by integration the amount of parabolic image movement, a_α, for a point off-axis, at an angle α, as

$$a_\alpha = \left[\frac{1}{2}\left(\frac{v}{h}\right)\dot{x}_f \sin\beta + \frac{1}{2}\dot{\beta}\dot{x}_f \tan\alpha\right] t_e^2. \tag{43}$$

Comparing equation (43) with equation (15), it is clear that the magnitude of off-axis motion is greater than axial motion, but it remains parabolic; and thus its modulation transfer may be evaluated by means of equation (28) or Figure 5.

Conclusions

The transfer function for image-motion arising from the finite slit-width of transverse-scanning panoramic cameras has been derived and investigated, subject to the assumption of small angular slit-width. This motion degrades the system's resolution in the direction perpendicular to the scan.

The contrast loss depends on the sine of the scan-angle, so nadir and near-vertical photography is not likely to be affected although the contrast loss at high-oblique angles can be very large. Furthermore, reducing either the film's transport velocity or its exposure time will always increase the modulation transfer. Contrast loss also depends on the v/h rate, but this is not under the designer's control. Finally, it was shown that the amount of image-motion is greater for points off the optical axis than for points on axis.

Acknowledgements

The author has benefited from many helpful comments by colleagues at The Perkin-Elmer Corporation, especially those of Cran H. Barrow and Richard C. Babish.

*Environmental Effects of Supersonic and Hypersonic Speeds on Aerial Photography**

JACK N. NIELSEN, *Applied Mechanics Div. Director* *and*

FREDERICK K. GOODWIN, *Special Staff Scientist, Vidya, Inc.*†

ABSTRACT: *Certain environmental effects may degrade the quality of photography taken from vehicles flying at supersonic and hypersonic speeds. Among those associated with the immediate environment of the vehicle are: (1) Metric distortion caused by refraction of light rays by flow field surrounding the vehicle; (2) Loss of resolution by scattering of light by turbulent boundary layers over the camera window; (3) Loss of contrast between ground object and its background by presence of luminous air in flow field; and (4) Metric distortion caused by temperature-induced window curvature. In addition to the above environmental effects, Rayleigh scattering between the ground and the vehicle can cause large reductions in contrast. This effect was also taken into account in determining the additional reduction in contrast caused by the luminous air in the flow field.*

Introduction

In recent years, much evidence has arisen to indicate that important effects of the aerodynamic and thermodynamic environments can occur in aerial photography taken for mapping or reconnaissance purposes at supersonic or hypersonic speeds. For instance, photography taken in the F101 airplane at

* Presented at the Society's 27th Annual Meeting, The Shoreham Hotel, Washington, D. C., March 19–22, 1961.

† 2626 Hanover St., Palo Alto, Calif.